Advances in Natural Sciences, Vol. 5, No. 4 (2004) (423-430)

NANOFLUIDIC COMPONENTS FOR ELECTROKINETIC MICROPUMPS

Henrik Bruus, Anders Brask, and Jörg P. Kutter

MIC – Department of Micro and Nanotechnology, DTU bldg. 345 east

Technical University of Denmark, DK-2800 Kongens Lyngby, Denmark

Abstract. We present the basic theory, fabrication, and test of a new design for an electrokinetic pump relying on electroosmosis in a nanofluidic component, a so-called porous frit. We demonstrate that our design provides long-term stability (up to two hours) under continuous operation and realistic working conditions (flow rates $Q \simeq 0.5$ μL/s and backpressures $p \simeq 10$ kPa). The remarkable stability of the pump is achieved by adding a new microfluidic component to the pump that controls the boundary diffusion layers influencing the electrokinetic processes essential for the pumping mechanism. Based on theoretical considerations we also discuss a novel current feedback system that allows for controlling the pump such that a nearly constant flow rate is obtained independent of varying backpressures.

I. INTRODUCTION

The field of lab-on-a-chip systems is evolving rapidly these years. Chips with many integrated bio/chemical, optical, electrical and mechanical functions have been developed. However, the problem of developing a reliable on-chip micro-pump has not been solved fully. One promising class of micro-pumps for microfluidic applications is the electrokinetic pumps, due to their integrability and compatibility with conventional microtechnology. Moreover they can produce a pulse-free flow without containing any moving parts [1, 2, 3].

In this paper we present a summary of our work on such electrokinetic micropumps, and in particular we focus on frit-based electroosmotic (EO) micropumps [4, 5]. The active components in these pumps are the so-called frits that contain a large number of parallel nanofluidic chanels [6]. Because the channels have small diameters (100 nm), they can sustain large pressures (10 kPa), and because there are so many in parallel, the flow rate through the frit is relatively high (0.5 μL/s). Stable operation of EO micropumps is highly wanted for use in many microfluidic systems. However, the majority of EO pumps studied so far are only working under idealized operating conditions, such as short operation periods and using continuous flushing. Under realistic load conditions EO pumps often fail over time mainly due to unstable electrochemical conditions such as varying pH levels and bubble formation induced by electrode reactions. We have achieved a remarkable stability of our pump by adding a new microfluidic component to the pump that controls the boundary diffusion layers influencing the electrokinetic processes essential for the pumping mechanism.

The stability of our pump has allowed us to determine a linear dependence on the electric current through the pump as a function of flow rate. This opens up for the possibility to add further stability to the pump by controlling the flow rate through a feedback system based on the electrical current: If the hydraulic backpressure of the system

changes so will the flow rate. This will induce a change in the current, which is easily monitored. By maintaining a fixed electrical current the fluctuations in the flow rate will be kept at a minimum. We sketch the theory of how to control the flow rate with the current by optimizing the size of the submicron pores in the frit.

II. BASIC THEORY OF ELECTROOSMOTIC FLOW

Consider, as in Fig. 1, a cylindrical channel in (r, θ, z)-coordinates of radius a filled with some buffer liquid with viscosity η and dielectric constant ϵ. Ions of symmetric valence Z are present in concentrations $c_+(r)$ and $c_-(r)$. Chemical charge-transfer processes at the wall spawn an electric potential ζ, the so-called zeta potential, adjacent to the walls and lead to a potential $\phi(r)$ in the liquid. Given the boundary conditions $\phi(a) = \zeta$ and $\phi'(0) = 0$ we find $\phi(r)$ and $c_\pm(r)$ by standard numerical methods as self-consistent solutions to the Poisson-Boltzmann equation [7]. It turns out that the potential $\phi(r)$ decays over a length scale, which is denoted the Debye length λ_D,

$$\lambda_D = \sqrt{\frac{\varepsilon k_{\mathrm{B}} T}{2e^2 Z^2 c}} \approx 10 \text{ nm}. \tag{1}$$

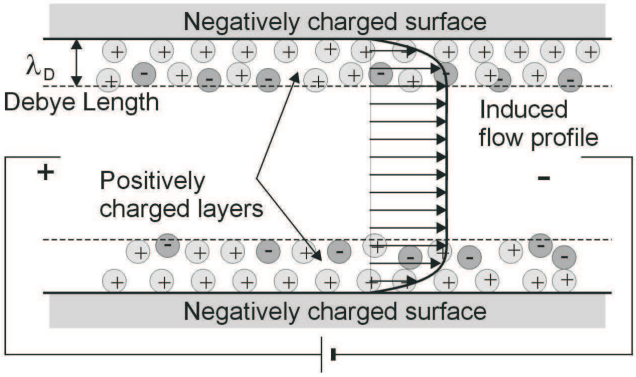

Fig. 1. The principle of electroosmotic flow in a cylindrical microchannel. Charge transfer processes at the wall leaves the wall and the liquid oppositely charged. Ions in the liquid is attracted towards the wall, and this charged liquid layer can then be moved by inserting biased electrodes at each end of the channel. By viscous drag the bulk of the liquid follows the motion of the charged suface layer, and an almost constant velocity profile results.

For a given electric field E_z and pressure gradient $\nabla_z p$ imposed in the z direction the velocity field $u(r)$ is found by solving the Navier-Stokes equation. When $E_z = 0$, $u(r)$ is the Poiseuille flow $u_{\mathrm{p}}(r, \nabla_z p) = -\nabla_z p\,(a^2 - r^2)/4\eta$ and, when $\nabla_z p = 0$, $u(r)$ is the Helmholtz-Smoluchowski flow $u_{\mathrm{eo}}(r, E_z) = \mu_{\mathrm{eo}}(1 - \phi(r)/\zeta)\,E_z$, where $\mu_{\mathrm{eo}} = -\epsilon\zeta/\eta$ is the electroosmotic mobility.

By integration the flow rate Q is found to be

$$Q(E_z, \nabla_z p) = \int_0^a 2\pi r \Big[u_{\mathrm{eo}}(r, E_z) + u_{\mathrm{p}}(r, \nabla_z p)\Big] dr. \tag{2}$$

In the case of pure Poiseuille flow with the flow rate is $Q_{\text{Poise}} = \pi a^4 \nabla_z p/(8\eta)$, while in the case of pure EO flow for $\lambda_D \ll a$ the flow rate is

$$Q_{\text{eo}} \approx \pi a^2 \mu_{\text{eo}} E_z, \quad \lambda_D \ll a. \tag{3}$$

The maximal pressure drop $p_{\max}$ that the EO pump can sustain, is given by the condition that the forward EO flow is cancelled by the backpressure-induced backflow, $Q_{\text{Poise}} = Q_{\text{eo}}$, which yields,

$$p_{\max} = \frac{8\eta L}{a^2}\, \mu_{\text{eo}} E_z, \quad \lambda_D \ll a. \tag{4}$$

From Eqs. (3) and (4) we learn that to obtain a high pressure capability we must take the channel radius as small as possible, but this will imply a very low flow rate. The way to have high values for both $p_{\max}$ and Q_{eo} is to take a huge number of narrow channel in a parallel coupling. This is exactly what is done by using a frit.

III. DESIGN OF THE FRIT-BASED EO PUMP

We can use the theory of Sec. 2 if we approximate the porous material with a bundle of parallel channels of radius a. This approximation may appear crude given the scanning electron micrograph shown in the left panel of Fig. 2 of the surface of one of the frits used in our experiments, but it nevertheless contains the right physics.

Fig. 2. Left panel: A scanning electron micrograph of one of the frits used in our experiments. In the top left corner is a 2 μm length bar. The frit consists of a collection of irregularly shaped glass beads (light gray) that are sintered together. The voids (dark gray/black) between the beads are the micro and nanofluidic channels in which the electroosmosis takes place. Right panel: the assembled pump of size 20 mm×20 mm×10 mm running on 30 V and yielding a flow rate of 0.5 μL/s and a backpressure of 10 kPa.

The right panel of Fig. 2 shows the assembled pump consisting of several layers of polymer sheets surrounding the central layer containing the frit. The actual design of the pump is shown in Fig. 3. It consists of an assembly of eleven polymer layers. The electrode

compartments α at the edges of the pump are separated from the frit compartment in the center by anion exchange membranes (AEM), which allow only negative ions to pass while bulk fluid and positive ions are retained. The pressure buildup generated by the frit is therefore confined to the inner loop of the pump, hence free ventilation of electrolytic gases developed at the electrodes in the outer loop is possible. The pumping stability is governed by the pH in the inner loop.

At the anode the pH will tend to drop because of the hydronium ions (solvated H^+) generated. A low pH will effectively remove the surface charge in the frit and thus stop the electroosmotic flow. It is therefore important that an AEM is used to prevent that hydronium ions are transported into the inner loop where the pumping takes place. Since hydronium ions will be blocked by the AEM to some degree most of the electrical current will be transported by hydroxyl ions (OH^-) that migrate from the cathode to the anode. An ion exchange membrane can only support a certain level of current density i. If the current density becomes higher than the limiting current density i_{limit} defined below, dissociation of water will happen on the surface (frit side) of the membrane. This reaction will increase the hydronium ion concentration in the frit.

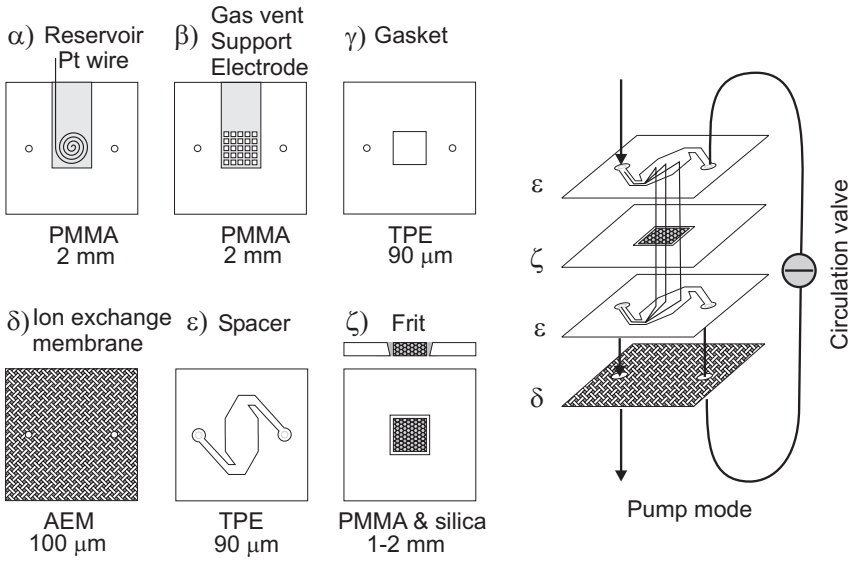

Fig. 3. (a) Modular design of the pump consisting of eleven layers assembled in the order $|\alpha|\beta|\gamma|\delta|\epsilon|\zeta|\epsilon|\delta|\gamma|\beta|\alpha|$. (b) The new fluidic component is the spacer ϵ that ensures a stable thickness of the diffusion boundary layer, and hence a stable operation of the pump, by continuous flushing of the membrane during operation. The total pump size is 20 mm×20 mm×10 mm. The circulation valve is external and used for initial filling and extracting samples for pH measurements.

$$i_{\text{limit}} = Z_-\Big(1 + \frac{Z_-}{Z_+}\Big) F D_- \frac{c_{\text{bulk}}}{\ell}, \tag{5}$$

where Z_- and Z_+ are the charge coefficients of the anion and cation species, ℓ is the

diffusion boundary layer thickness, D_- is the diffusion coefficient of the anions, F is the Faraday constant, and c_{bulk} is the concentration of the buffer. The current density should therefore not exceed the limiting current density considerably. To ensure a high limiting current density the diffusion layer thickness is reduced by adding a new microfluidic component, namely the spacer layer marked ε in Fig. 3, which forces the liquid from the inlet to flow across the ion exchange membrane. The thickness of the diffusion boundary layer surrounding the membrane is kept small by this flow. Furthermore, when the pump is generating flow, the buffer is replenished continuously. One mole of buffer can absorb two moles of hydronium before any substantial pH change. The stability of the pH value and hence the efficiency of the pump is compromised only if the flow is significantly reduced by a high backpressure. A slow flow will increase the diffusion boundary layer thickness ℓ and subsequently deplete the buffer in the inner loop.

Table 1. *A table listing the main properties of the two frits A and B used in the two EO pumps studied in this paper.*

	Frit A	Frit B
Material	Borosilicate	Silicate 99.99%
Pore size	1.3 μm	200 nm
Shape	Circular	Square
Area	$\pi(1.8\text{ mm})^2 = 10\text{ mm}^2$	$(5\text{ mm})^2 = 25\text{ mm}^2$
Thickness	2 mm	1 mm
Borate buffer	5 mM	100 mM
pH level	9.0	9.2

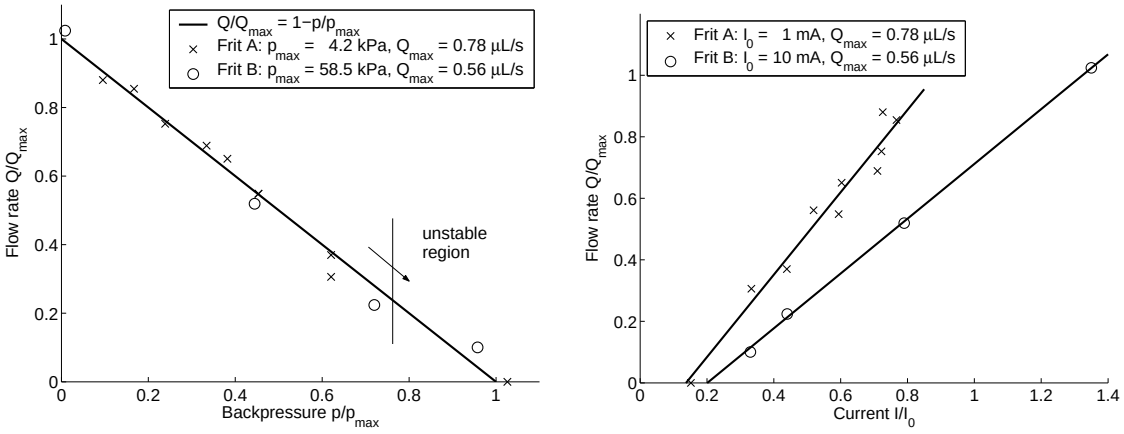

Fig. 4. (a) Continuous measurements of the normalized flow rate $Q/Q_{\max}$ versus the normalized backpressure $p/p_{\max}$ for frit A and B with pore sizes 1.3 mm and 200 nm, respectively. The applied voltage was 30 V in both cases. (b) Continuous measurements of flow rate Q and current I at different backpressure. Same series as in panel (a). The total operation time in this experiment was 2 hours without degrading performance. However, there exists a critical Q/I ratio where the pump becomes unstable. This ratio will be reached near the maximum backpressure capability of the pump.

IV. EXPERIMENTAL METHODS, RESULTS AND DISCUSSION

Flow rates were measured by collecting liquid in a pressurized reservoir placed on a balance (0.1 mg precision). The reservoir pressure (backpressure) was controlled by a N_2 source and measured by two pressure sensors (0-150 psi, 0-10 bar). Suspended flexible silicone tubing was used to connect the collecting reservoir in order to avoid interference with the balance. The data (time, pressures, mass, current, voltage) was collected using a data acquisition card in a PC. pH levels were measured by four color pH indicators.

We have tested two types of frits, A and B, see Table 1. Such frits result in large flow rates while at the same time having a large pressure capability.

The pump characteristics measured in the tests of pump A and B are shown in Fig. 4(a). The flow rate is seen to decrease linearly as the backpressure is increased. Due to electrolysis in the outer loop, the reservoirs a in Fig. 3(a) need to be refilled after several hours of use. The long-term stability for pumps A and B has been observed for 15 min and 30 min, respectively, at specific backpressures. Operating continuously with various loads the pump did not show any signs of degrading performance over a period of 2 hours.

V. THEORY OF CURRENT FEEDBACK FOR FLOW CONTROL

The linear I-Q dependence shown in Fig. 4(b) allows for a feedback loop where the EO voltage driving the pump (and thus Q) can be regulated by the electric current. In the following we shall give the theoretical arguments for that statement.

The electric current density in the channel is a sum of the ordinary ionic electromigration governed by the electrophoretic mobility $\mu_{\rm ep}$ and, because of charge imbalance, the convection of ions. The current I is found by integration of this current density,

$$\begin{aligned} I(E_z,\nabla_z p) = FZ\int_0^a 2\pi r\left\{\left[c_+(r)+c_-(r)\right]\mu_{\rm ep}E_z+\left[c_+(r)-c_-(r)\right]u_{\rm eo}(r,E_z)\right\}dr \\ + FZ\int_0^a 2\pi r\left\{\left[c_+(r)-c_-(r)\right]u_{\rm p}(r,\nabla_z p)\right\}dr. \end{aligned} \tag{6}$$

Recalling that $u_{\rm eo}\propto E_z$ and $u_{\rm p}\propto\nabla_z p$, Eqs. (2) and (6) can be written as linear functions of E_z and $\nabla_z p$. By introducing the constants β_E, β_p, γ_E, and γ_p we find

$$Q(E_z,\nabla_z p) = \gamma_E E_z - \gamma_p\,\nabla_z p, \tag{7}$$

$$I(E_z,\nabla_z p) = \beta_E E_z - \beta_p\,\nabla_z p. \tag{8}$$

We base our flow regulator theory on these linear equations. Let E_z^0 be a reference field, and calculate for $\nabla_z p = 0$ the corresponding current $I^0\equiv\beta_E E_z^0$ and flow rate $Q^0\equiv\gamma_E E_z^0$. For fixed E_z^0 an applied backpressure $\nabla_z p$ will reduce Q from Q^0 linearly with slope $-\gamma_p$,

$$Q(E_z^0,p) = Q^0 - \gamma_p\,\nabla_z p. \tag{9}$$

From this we find the so-called electroosmotic pressure $\nabla_z p_{\rm eo}^0 = Q^0/\gamma_p$, which is the backpressure gradient that makes the flow rate zero, $Q(E_z^0,\nabla_z p_{\rm eo}^0)=0$.

Now we allow for changes in E_z. In particular we define E_z^p as the field that for a given backpressure gradient $\nabla_z p$ maintains the current at the original value I^0, i.e., $I(E_z^p, \nabla_z p) = I(E_z^0, 0)$, which can be solved to yield

$$E_z^p = E_z^0 + \frac{\beta_p}{\beta_E} \nabla_z p. \tag{10}$$

Upon insertion of E_z^p and into Eq. (7) we obtain a new linear function for Q,

$$Q(E_z^p, p) = Q_0 - \Gamma_p \nabla_z p, \quad \text{where } \Gamma_p = \gamma_p - \frac{\beta_p}{\beta_E} \gamma_E. \tag{11}$$

Thus by applying a simple current feedback that keeps the electric current I constant by changing E_z, the Q-p slope can be reduced from γ_p to Γ_p, thereby keeping the backpressure-induced loss in the flow rate Q to a minimum. The new slope Γ_p also changes the backpressure capacity,

$$\nabla_z p_{\text{eo}}^p = \nabla_z p_{\text{eo}}^0 \left(\Gamma_p / \gamma_p\right)^{-1}. \tag{12}$$

Note that regardless of this change in backpressure capacity the pump efficiency measured as $\nabla_z p / E_z$ remains unchanged. Fig. 5 shows Γ_p / γ_p as a function of the Debye length λ_D and the mobilities μ_{eo} and μ_{ep}. Perfect flow control corresponds to $\Gamma_p = 0$ equivalent of infinite backpressure capacity. Clearly, this can not be achieved, but from Fig. 4(a) we can see that a Γ_p can be minimized by proper choice of the radius a of the pores in the frit, namely $\lambda_D / a \approx 0.4$, or $a \approx 25$ nm.

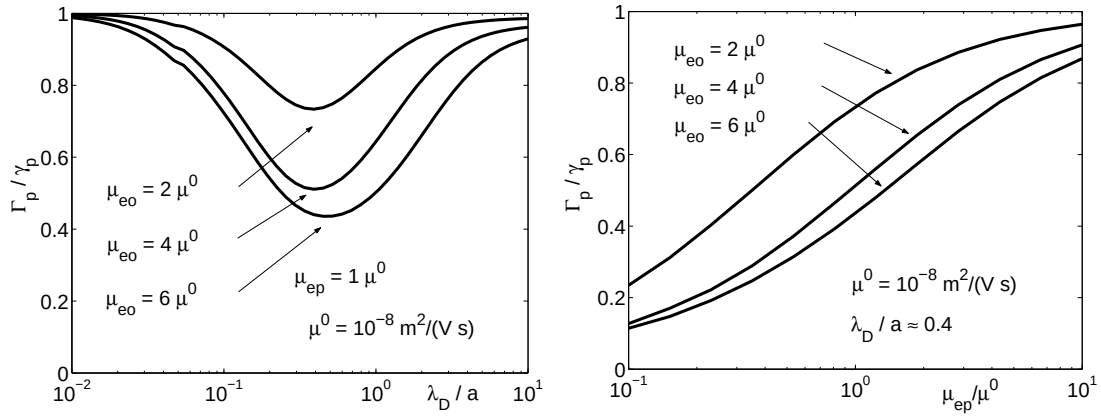

Fig. 5. (a) The slope $\Gamma_p = dQ/d\nabla_z p$ as a function of λ_D/a and μ_{eo}. The mobilities are given in units of $\mu^0 = 10^{-8}\text{m}^2/(\text{V s})$. (b) Γ_p as a function of μ_{ep} for $\lambda_D/a \approx 0.4$, which is the value in diagram (a) that minimizes Γ_p.

VI. CONCLUSION

A stable stand-alone micropump based on nanofluidic frits has been developed and tested successfully. The design is highly versatile and can be modified by choosing the

proper frits to meet most flow requirements in microfluidic applications. Disadvantages are the dependence on the pumping liquid and development of electrolytic gases. The inline EO pump is simple in its construction and delivers a precise and stable flow.

As shown in Fig. 4(b) the long-term stability of our pump allowed for measuring and establishing the linear relation between I and Q. This is a first step towards realizing the novel current feedback system that we have presented and analyzed in Sec. 5. The optimum ratio for flow regulation was found to be $\lambda_D/a \approx 0.4$, which for normal values of λ_D implies that the optimal pore size in the nanofluidic component shoul be in the range 10 - 100 nm.

Acknowledgments. This work is partly supported by the Danish Technical Research Council, μTAS Frame Program Grant No. 26-00-0220.

REFERENCES

1. Y. Takamura, H. Onoda, H. Inokuchi, S. Adachi, A. Oki, Y. Horiike, Proc. μTAS 2001, Monterey (CA), USA, October 2001, p. 230-232
2. W. E. Morf, O. T. Guenat, N. F. d Rooij, Sens. Actuators B Chem. **72** 266 (2001)
3. D. J. Laser, J. G. Santiago, A review of micropumps, J. Micromech. Microeng. **14** R35-R64 (2004)
4. A. Brask, H. Bruus, and J. Kutter, Proceedings of microTAS 2003, Lake Taho, USA, October 2003, vol. 1 pp. 223-226
5. A. Brask, H. Bruus, and J. Kutter, Proceedings of microTAS 2004, Malmo, Sweden, September 2004, vol. 2 p. 136-138
6. S. Yao, D. Huber, J.C. Mikkelsen, and J.G. Santiago, Proceedings of IMECE 2001, New York (NY).
7. R.F. Probstein, *Physiochemical Hydrodynamics. An introduction*, John Wiley and Sons, MIT (2nd ed., 1994).

Received October 27, 2004